1-1-2010

Preparation of titanium dioxide nanoparticles from electrocoagulated sludge using sacrificial titanium electrodes

H K. Shon
University of Technology, Sydney, hkshon@enguts.edu.au

S Phuntsho
University of Technology, Sydney

S Vigneswaran
University of Technology, Sydney

Jaya Kandasamy
University of Technology, Sydney

Long Nghiem
University of Wollongong, longn@uow.edu.au

See next page for additional authors

Environ. Sci. Technol. **2010,** *44,* 5553–5557

Preparation of Titanium Dioxide Nanoparticles from Electrocoagulated Sludge using Sacrificial Titanium Electrodes

H. K. SHON,*,† S. PHUNTSHO,† S. VIGNESWARAN,† J. KANDASAMY,† L. D. NGHIEM,‡ G. J. KIM,§ J. B. KIM,∥,⊥ AND J.-H. KIM∥,⊥

Faculty of Engineering, University of Technology, Sydney (UTS), P.O. Box 123, Broadway, NSW 2007, Australia, School of Civil Mining and Environmental Engineering, The University of Wollongong, Wollongong, NSW 2522, Australia, Department of Chemical Engineering, 253 Yonghyun-dong, Nam-gu, Inha University, Incheon, 402-751, Korea, Photo & Environmental Technology Co. Ltd., Gwangju 500-460, and Korea, School of Applied Chemical Engineering & The Institute for Catalysis Research, Chonnam National University, Gwangju 500-7 57, Korea, Chonnam National University, Gwangju 500-757, Korea

Received January 29, 2010. Revised manuscript received May 29, 2010. Accepted June 4, 2010.

A comprehensive investigation of electrocoagulation using sacrificial titanium (Ti) electrodes in wastewater was carried out. The effects of specific process variables, such as initial pH, mixing, current density, initial organic loading, and ionic/electrolyte strength were first optimized to produce recyclable Ti-based sludge. The sludge was incinerated at 600 °C to produce functional TiO_2 photocatalyst. X-ray diffraction analysis revealed that TiO_2 produced at optimum electrocoagulation conditions was mostly anatase structure. The specific surface area of the synthesized TiO_2 photocatalyst was higher than that of the commercially available and widely used Degussa P-25 TiO_2. Furthermore, energy dispersive X-ray and X-ray photoelectron spectroscopy analyses showed that in additional to titanium and oxygen, this photocatalyst is also composed of carbon and phosphorus. These elements were mainly doped as a substitute site for the oxygen atom. Transmission electron microscopy images exhibited sharply edged nanorods, round nanoparticles, and nanotubes with nonuniform shapes showing some structural defects. Photodecomposition of gaseous acetaldehyde by this photocatalyst was also conducted under UV and visible light irradiation to study the photocatalytic properties of the doped TiO_2 photocatalyst. While no photocatalytic activity was observed under visible light irradiation, this doped TiO_2 photocatalyst exhibited high photocatalytic activity under UV light.

* Corresponding author phone: +61295142629; fax: +61295142633); e-mail: hkshon@eng.uts.edu.au.
† University of Technology, Sydney (UTS).
‡ The University of Wollongong.
§ Inha University.
∥ Photo & Environmental Technology Co. Ltd.
⊥ Chonnam National University.

Introduction

As fresh water resources become scarcer, wastewater reuse and desalination are increasingly being utilized as part of sustainable water management programs. At the same time, drinking water standards for protecting public health are becoming ever more stringent. To meet these new standards, many alternative options for water and wastewater treatment are being investigated. Electrocoagulation, for example, has been widely considered for its simplicity in design, high separating efficiency, ease of operation and automation (*1*). Electrocoagulation can be utilized to treat wastewater from a range of sources including domestic, tannery, palm oil mill, oil−water emulsion, mining, dye and textile, and food processing (*1*−*8*). Given its simplicity in design and operation, electrocoagulation has promising potential for decentralized wastewater treatment applications (*9*).

Removal mechanisms in an electrocoagulation process include coagulation, adsorption, precipitation, and floatation (*1, 10*−*12*). To optimize its operating parameters, the effects of pH, electrodes, current density, reactor design, supporting electrolyte concentration, solution temperature, and pollutant compound and concentration must be carefully considered (*1, 13*−*16*). Electrodes, current density, and pH have been identified as key operational parameters influencing pollutant removal mechanism.

Dedicated efforts have been made on the development of novel electrodes, which is the most important part of an electrocoagulation unit, to improve performance (*13*). The authors of refs *1 and 13* compared different anodes, such as graphite, Pt, PbO_2, IrO_2, SnO_2−Sb_2O_5, IrO_x, RuO_2, and TiO_2 in their reviews. However, most current electrocoagulation applications still use the conventional aluminum or iron anodes (*1*). Although these conventional electrode materials can offer high coagulation efficiency, they both generate high O_2 evolution overpotential and are anodically soluble with low durability (*17*). Reports on novel electrodes materials remain very scarce in the literature.

Similar to chemical coagulation, electrocoagulation also produces a large amount of chemical sludge that requires further management. Disposal of chemical sludge to landfill could cause secondary contamination. To reduce the environmental impact from sludge disposal, Shon et al. (*18*) developed a novel method to produce alumina (Al_2O_3), hematite (Fe_2O_3), and titanium oxide (TiO_2) nanoparticles from Al-, Fe-, and Ti-coagulated sludge respectively. Of all, TiO_2 is the most widely used metal oxide in the manufacture of cosmetics, paints, electronic paper, solar cells, and other environmental applications (*19*−*21*). On the other hand, TiO_2 nanotubes are also attracting great interest because of their high surface-to-volume ratios and size-dependent properties. Among the several methods for preparing TiO_2 nanotubes, titanium electrochemical anodization is regarded as a relatively convenient method to prepare highly ordered TiO_2 nanotube structure. The preparation method of TiO_2 nanotube arrays via anodic oxidation of titanium foil in a fluoride-based solution was first reported by Gong et al. (*22*). The factors affecting the anodization include electrolyte solution/concentration, pH, voltage, and temperature (*23*). Electrolyte composition plays a crucial role in determining the resultant nanotubes.

The use of TiO_2 in a wide range of applications means that the demand for this metal oxide is increasing rapidly. The demand could partially be met by TiO_2 produced from Ti-coagulated sludge which has been found to be superior to the commercially available TiO_2 (P-25) in both photo-

10.1021/es100333s
Published on Web 06/18/2010

catalytic activity and surface area (*24*). The same concept can be applied to Ti-electrocoagulation not only to reduce the sludge production but also to generate reusable sludge offering a novel solution to many environmental and economic issues associated with sludge handling.

No previous studies have attempted to comprehensively investigate electrocoagulation using sacrificial Ti electrodes. Therefore, this study aims to provide a holistic assessment of titanium as a novel electrode material. Specific process variables of electrocoagulation with Ti electrodes were systematically optimized. These process variables included initial pH, mixing rate, current density, initial organic loading and ionic/electrolyte strength. The optimum operating conditions were applied to produce a large amount of recyclable sludge. The sludge was incinerated at 600 °C to produce a TiO_2 photocatalyst. Subsequently, photocatalytic properties of the synthesized TiO_2 were examined in detail.

Experimental Section

Synthetic Wastewater. Synthetic wastewater (SWW) was prepared with a wide range of organic molecular sizes, representing effluent organic matter generally found in biologically treated sewage effluent. The detailed constituents are provided elsewhere (*25, 26*).

Electrocoagulation. The basic premise of electrocoagulation is the production of a coagulant via electrolysis. By applying electric current to titanium electrode plates, titanium ions from the anode plate are dissolved into the aqueous solution. Hydrogen gas is released at the cathode which causes the flotation. The electrode reactions using titanium are as follows:

Anode

$$Ti_{(s)} \rightarrow Ti^{4+} + 4e^- \quad (1)$$

Cathode

$$4H_2O + 4e^- \rightarrow 2H_{2(g)} + 4OH^- \quad (2)$$

The Ti^{4+} ions formed are hydrolyzed and subsequently generate titanium hydroxides and polyhydroxides (*27*). In the process, water is also electrolyzed in a parallel reaction, generating oxygen at the anode and hydrogen at the cathode. These gases destabilize the contaminants, such as colloids, suspended solids, organic matter, heavy metals, microorganisms, and phosphorus. The aggregation of destabilized particles occurs, followed by separable precipitation/flotation of the aggregated flocs. The precipitation or flotation of flocs result in the purification of wastewater.

The electrocoagulation reactor used in this study consisted of a 6 L pyrex glass beaker with a capacity of 5 L, 4 titanium electrodes (23 cm ×9 cm ×0.3 cm) in a monopolar configuration, and a DC power converter (Q1770, Dick Smith Electronics, Australia). Prior to each test, 5 L of synthetic wastewater was introduced to the electrocoagulation cell. The current was varied in the range of 1−2.5 A, and the voltage was set constant at 30 V. When not in use, the titanium electrodes were immersed in acid bath (1 M HCl) and prior to each experiment, they were carefully cleaned using steel wool to remove any titanium oxide that may have formed on the surface.

Analysis of Water Sample. The sampling during electrocoagulation was carried out at regular time intervals. Organic carbon was measured using a Dohrmann Phoenix 8000 UV-persulphate TOC analyzer equipped with an auto sampler. All samples were filtered through 0.45 μm membrane prior to organic measurement. The molecular weight (MW) distribution of organics was determined using high-pressure size exclusion chromatography (HPSEC, Shimadzu Corp., Japan) with a SEC column (Proteinpak 125, Waters Milford, U.S.A.). Polystyrene sulfonates (PSS 210, 1800, 4600, 8000, and 18000 Da) were used as standards to calibrate the equipment.

TABLE 1. Optimum Parameters for Ti-Based Electrocoagulation

parameters	range tested	optimum value
current density (mA/cm^2)	3.3−8.3	8.3
agitation speed (rpm)	80−1500	700
initial pH	4−12	4
initial organic loading (mg/L)	5−50	no effect

Characterization of TiO_2. XRD images (Rigaku, Japan) were used to investigate and identify the structure of anatase and rutile TiO_2 photocatalysts. All the XRD patterns were analyzed with MDI Jade 5.0 (Materials Data Inc., U.S.A.). UV−vis-NIR spectrophotometer (Cary 500 Scan, Varian, U.S.A.) was used to identify the absorbance range. XPS measurements were performed with a Leybold LHS10 spectrometer, equipped with a twin anode (Mg Kα/Al Kα) nonmonochromatized source (operated at 280 W) and a hemispherical electron analyzer. SEM and TEM (Rigaku, Japan) images were used to investigate the microscopic shapes and sizes of TiO_2. Micromeritics Gemini 2360 analyzer (U.S.A.) with automatic surface area analyzer was used for BET surface area analysis. For investigating the photocatalytic activity of the TiO_2 produced from sludge, a cuboid stainless steel (Top-face quartz, volume 3.8 L) airtight reactor was used to study the adsorption and photocatalytic oxidation of acetaldehyde over UVA-illuminated catalysts. The reactor was topped with two 10 W, 352 nm UVA lamps (Sankyo Denki, F10T8BL, Japan) and had three rubber openings for the injection of acetaldehyde, air mixing inside the reactor and for withdrawal of samples. The last opening was connected to a gas chromatograph/flame ionization detector (GC/FID) (*hp*5890 series II, Wilmington, U.S.A.) for measuring variations in acetaldehyde concentration. The reaction took place at room temperature of 24 °C for 120 min (60 min adsorption and 60 min photodecomposition). Photocatalysts were uniformly sprinkled on a glass Petri-dish (9 cm of diameter) and placed at a distance of 10 cm from UVA lamps in the center of the reactor. The reaction began after closing the reactor door and injecting acetaldehyde (Stem Supply, SA, Australia) through the injection cavity using an airtight syringe. The concentration of acetaldehyde was recorded at fixed intervals for adsorption and photocatalysis. A detailed protocol of acetaldehyde oxidation using TiO_2 can be found elsewhere (*28*).

Results and Discussion

Optimum Operating Conditions for Electrocoagulation. The effects of specific process variables, such as initial pH, mixing, current density, and the initial organic loading were first optimized to produce recyclable Ti-based sludge. The optimum values of each process variables shown in Table 1 are based on the highest removal of dissolved organic carbon. The details related to study on the optimum operating parameters are available in the Supporting Information (Figures S1−S6).

The optimum current density of 8.3 mA/cm^2 was in fact four times higher than that of Al or Fe electrodes, which require approximately 2 mA/cm^2 for a long period of operation (*1*). This is probably because of less dissolution of metal ions from the Ti sacrificial metal anode.

The influence of initial pH (range 4−12) indicated that the dissolved organic removal was quite low at a higher initial pH. Earlier studies have reported that electrocoagulation performed normally at slightly acidic to neutral pH because of the solubility of metal oxides (*1, 29−31*). The optimum pH

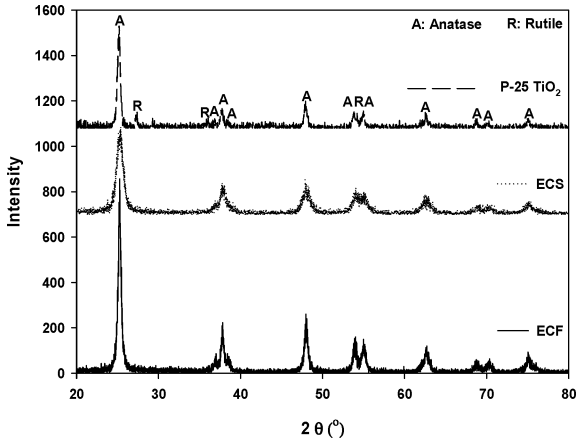

FIGURE 1. XRD image of ECF and ECS produced from electrocoagulation after incineration at 600 °C (A, anatase; R, rutile).

for the organic removal by Ti-electrocoagulation was observed to be 4. However, in most cases, the solution pH increased as electrocoagulation progressed because of continuous OH^- formation at the cathode as shown by eq 2 (*32*). When the initial organic concentration of SWW was high, the removal efficiency by electrocoagulation was lower during the early stages of electrolysis, but after 30 min, the removal efficiencies were similar regardless of the initial organic concentration.

Water conductivity is an important parameter for application of electrocoagulation in fresh water, brackish water, and seawater. A higher conductivity (ionic strength) generally causes an increase in current density at the same cell voltage or the cell voltage decreases with increase in water conductivity. The conductivity (ionic strength) of the wastewater used in this study was adjusted by adding NaCl. The organic removal efficiency with the Ti electrodes was slightly enhanced at higher ionic strength (Supporting Information, Figure S5).

The organic removal by electrocoagulation in terms of DOC under optimum parameters was between 60 and 70% (Supporting Information). Electrocoagulation removed a wide range of molecular weight distribution (MWD) of organic matter. The organic removal in terms of MWD suggests that that Ti-based electrocoagulation could remove much smaller MW compounds in comparison to chemical coagulation-flocculation (Supporting Information, Figure S6). Shon et al. (*24*) reported that the $TiCl_4$ coagulant removed some of the smaller MW compounds (860−1000 Da), while the smallest MW ranges of compounds of around 250 Da could not be removed.

Synthesis of TiO_2 from Sludge and Its Characterization. Electrocoagulation was performed at optimum operating conditions (pH 4, initial organic loading (C_0) = 10 mg/L, mixing rate =700 rpm, and current density =8.3 mA/cm^2), and the electrocoagulated sludge produced was collected. Two types of electrocoagulated sludge were collected separately: Ti-salt floc that floated on the water surface (ECF) and Ti-salt floc that settled at the bottom (ECS). This sludge was then incinerated at 600 °C to remove water content and organic substances. This temperature was found effective in producing functional nanoparticle from sludge containing water and organic matter and was adapted from Shon et al. (*24*). The detail characteristics of the anatase TiO_2 produced from ECS and ECF were studied using advanced analytical techniques as described below.

XRD Image and Surface Area. XRD patterns were used to identify the particle structures of the ECF and ECS, and their structures were compared with the commercially available P-25 TiO_2 (Figure 1). Both ECF and ECS exhibited only anatase structure, whereas P-25 TiO_2 showed both anatase and rutile structure. The transformation from anatase to rutile at ambient pressure was found to be at about 550 °C probably because of the impurities in the TiO_2 produced from the floated and settled floc. The crystallite size was calculated by Scherrer's formula based on XRD intensity (*33*). The crystallite sizes of the particles for ECF, ECS, and P-25 were 32, 21, and 24 nm, respectively (Table 2). The primary crystallization for ECS was smaller than that of ECF. This suggests that the ECS could have the smaller floc size and less impurity, which could lead to the production of smaller TiO_2 nanoparticles. In general, TiO_2 (P-25) does not have any pore size or pore volume so it is probably because of aggregated pore volume and pore size of the particles.

TABLE 2. Crystallite Size, BET Surface Area, Average Pore Diameter, and Pore Volume of ECF and ECS Produced from Electrocoagulated Sludge

	crystallite size (nm)	surface area (m^2/g)	average pore diameter (nm)	pore volume (cm^3/g)
ECF	32	60.4	7.4	0.29
ECS	21	136.4	5.6	0.36
P-25	24	42.3	6.1	0.46

The BET specific surface areas of both ECF and ECS were significantly higher than that of P-25 TiO_2. This result is in a good agreement with the crystallite size of ECF and ECS. The average pore diameter of ECF and ECS was 7.4 and 5.6 nm, respectively.

SEM/EDX Results. Figure 2 shows the SEM images of ECF and ECS photocatalysts. The SEM images show different size, shape and dimension of the aggregated particles. The majority of aggregated particles were found to be less than 50 nm. The aggregated size of ECF was larger than that of ECS.

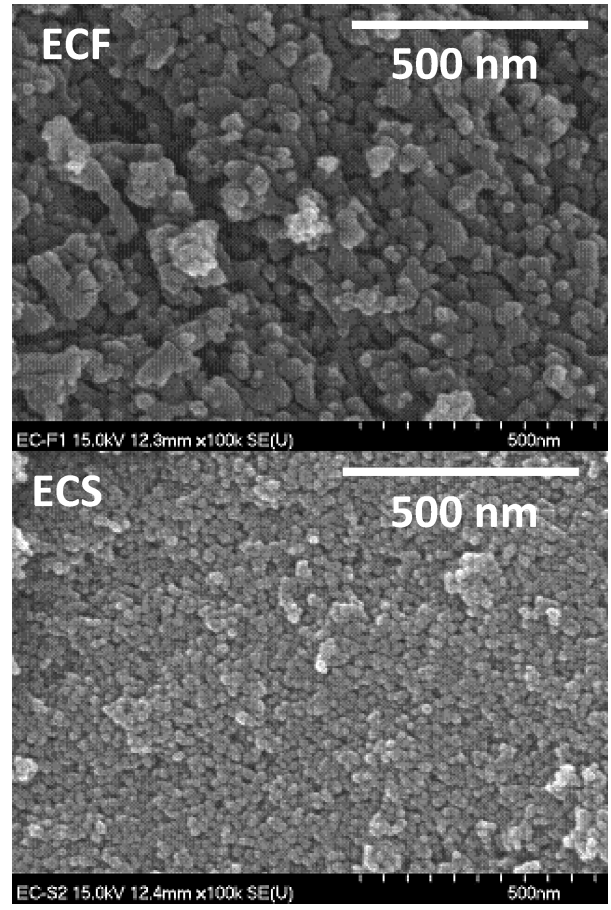

FIGURE 2. SEM images of ECF and ECS nanoparticles.

TABLE 3. Atomic (%) Fraction of Different Elements in ECF and ECS Powders after Incineration at 600 °C and P25

element	ECF (atomic %)	ECS (atomic %)	P-25 (atomic %)
C	11.09	9.97	
O	65.57	66.68	76
P	0.21	0.88	
Ti	22.31	21.28	23

EDX analysis was performed to determine the presence of the different elements in ECF, ECS, and P-25 (Table 3). The constitutive elements of ECF and ECS were mainly Ti, O, C, and P. The C atoms probably come from the remaining organic carbon of the coagulated organic matter. The P atom content was found to be high in ECS. The P in the SWW upon electrocoagulation gets incorporated into the flocs predominantly in the heavier flocs, which settle down. The atomic percentage of Ti, O, C and P in ECF, ECS, and P-25 are shown in Table 3. These results imply that in ECF and ECS, most of the C and P atoms were mainly doped as a substitute site for an O atom. The detailed valence states of Ti, O, C, and P are shown in Supporting Information, Figure S7.

TEM Results. TEM images of ECF and ECS photocatalysts in Figure 3 show sharply edged nanorods, round nanoparticles, and nanotubes. These structures were not uniform in shape showing structural defects and interconnections at certain sites. The nanorods had estimated dimensions of 5−10 nm in diameter and 20−50 nm in length, and the round nanoparticles consisted of close-packed and tube-type nanocrystals with sizes ranging from 10−100 nm. The nanotubes formation with discrete, hollow, cylindrical tube-like features included inner diameters of 20−80 nm, wall thickness of 10−30 nm, and lengths of 0.1−1 μm. The irregular size distribution of nanotubes may be the result of the high voltage applied (30 V) in this study. Mor et al. (*23*) reported that the nanotube structure at anodizing voltages greater than 23 V was lost with a sponge-like randomly porous structure. Compared to ECF, ECS photocatalyst had more nanotubes with different and bigger nanosize distributions. The nanorods and nanoparticles were probably from aggregated floc with the Ti^{4+} ions released from Ti electrodes, while the nanotubes might be from separated TiO_2 nanotube arrays via anodic oxidation of the titanium electrode.

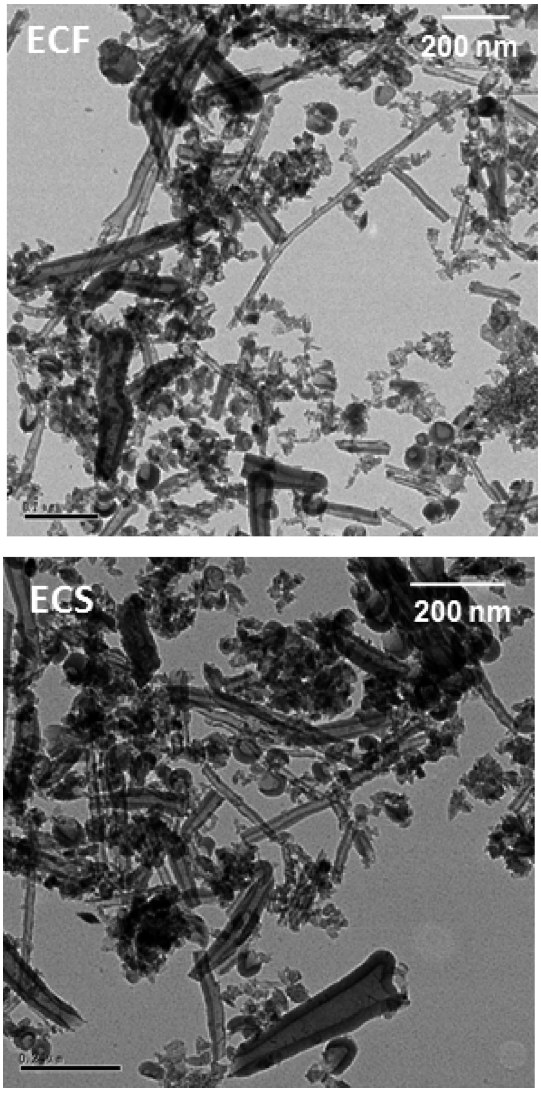

FIGURE 3. HR-TEM images of ECF and ECS nanoparticles.

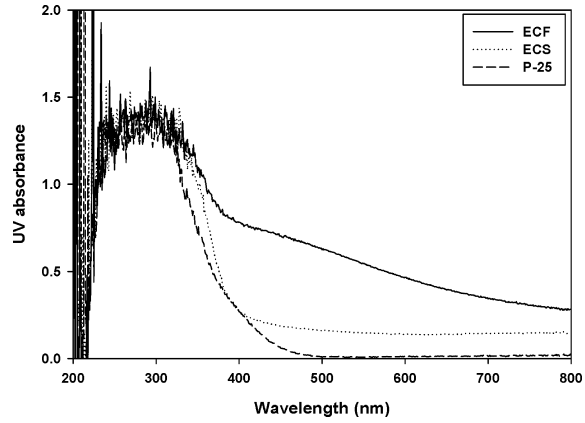

FIGURE 4. Optical absorbance of ECF and ECS photocatalysts.

UV−Vis Spectrophotometer. Carbon (C) doping can be used to generate visible light responsive TiO_2 (*34, 35*). The localized C (2p) formed above the valence band is the origin of visible light sensitivity, which leads to an inferior hydrophilic property when irradiating with visible light compared with UV light. The optical property of ECF and ECS photocatalysts was thus examined using the ultraviolet−visible−near-infrared spectrophotometer. It was observed that P-25 photocatalyst absorbed the majority of UV light (less than a 400 nm wavelength), while the ECF absorbed both UV light and visible light (Figure 4).

Photocatalytic Activity. The photodecomposition rate of acetaldehyde using the ECF and ECS photocatalysts under UV and visible light irridiation was compared to that of the commercially available P-25 photocatalyst (Figure 5). In the absence of light, ECS was found to have the highest adsorption capacity (up to 50% removal of acetaldehyde), while ECF and P-25 adsorbed only about 15% of acetaldehyde. The high adsorption removal with ECS suggests that the nanotubes with the larger surface area increase the interaction between acetaldehyde and ECS. The photodecompositions by ECS and P-25 under UV light irradiation after 200 min operation were 91.7% and 98.5%, respectively, whereas the photodecomposition with ECF was only 27.7%. However, under visible light (fluorescent light at 436 nm and a light power of 0.9 mW/cm^2) irradiation, none of the photocatalyst exhibited any photocatalytic activity (data not shown), although ECF showed visible light absorbance (Figure 5).

In summary, Ti-electrocoagulation of wastewater results in recyclable sludge. This treatment option not only solves the environmental issues associated with sludge disposal but also enhances the economy of wastewater treatment by producing a valuable photocatalyst as byproduct. Further process optimization could result in higher electrocoagulation efficiency. TiO_2 nanotubes with a high surface to

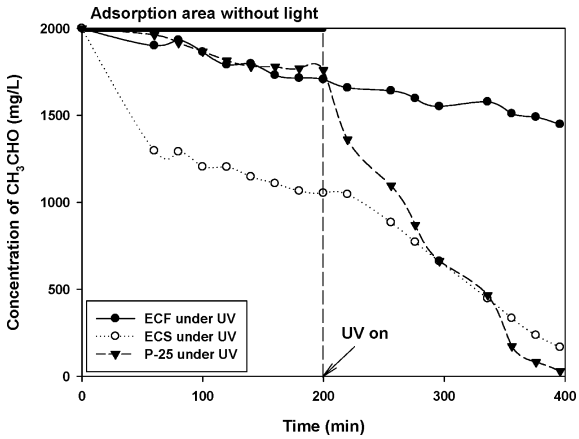

FIGURE 5. Variation of acetaldehyde (CH_3CHO) concentration with irradiation time (initial concentration of CH_3CHO, 2000 mg/L; UV irradiation, black light of three lamps of 10 W each).

volume ratio are obtained from the electrocoagulated sludge at lower temperature. The photocatalytic efficiency of this TiO_2 is comparable to the commercially available photocatalyst P-25. The simplicity in design and layout offered by electrocoagulation is what makes this method attractive for water and wastewater treatment.

Acknowledgments

This work was supported by an ARC grant and Priority Research Centers Program through the National Research Foundation of Korea (NRF) funded by the Ministry of Education, Science and Technology (2009-0094057) and the Center for Photonic Materials and Devices at Chonnam National University.

Supporting Information Available

Additional material as described in the text. This material is available free of charge via the Internet at http://pubs.acs.org.

Literature Cited

(1) Chen, G. Electrochemical technologies in wastewater treatment. *Sep. Purif. Technol.* **2004**, *38* (1), 11–41.
(2) Kurt, U.; Gonullu, M. T.; Ilhan, F.; Varinca, K. Treatment of domestic wastewater by electrocoagulation in a cell with Fe-Fe electrodes. *Environ. Eng. Sci.* **2008**, *25* (2), 153–161.
(3) Murugananthan, M.; Raju, G. B.; Prabhakar, S. Separation of pollutants from tannery effluents by electro flotation. *Sep. Purif. Technol.* **2004**, *40* (2004), 69–75.
(4) Emamjomeh, M. M.; Sivakumar, M. Review of pollutants removed by electrocoagulation and electrocoagulation/flotation processes. *J. Environ. Manage.* **2009**, *90* (2009), 1663–1679.
(5) Ho, C. C.; Chan, C. Y. The application of lead dioxide-coated titanium anode in the electroflotation of palm oil mill effluent. *Water Res.* **1986**, *20* (12), 1523–1527.
(6) Balmer, L. M.; Foulds, A. W. *Filtr. Sep.* **1986**, *23*, 366–369.
(7) Poon, C. P. C. Electroflotation for groundwater decontamination. *J. Hazard. Mater.* **1997**, *55* (1−3), 159–170.
(8) Hernlem, B. J.; Tsai, L. S. Chlorine generation and disinfection by electroflotation. *J. Food Sci.* **2000**, *65*, 834–837.
(9) Holt, P. K.; Barton, G. W.; Mitchell, C. A. The future for electrocoagulation as a localised water treatment technology. *Chemosphere* **2005**, *59* (2005), 355–367.
(10) Vlyssides, A. G.; Karlis, P. K.; Zorpas, A. A. Electrochemical oxidation of noncyanide stripperswastes. *Environ. Int.* **1999**, *25* (1999), 663–670.
(11) Grimm, J.; Bessarabov, D.; Sanderson, R. Review of electro-assisted methods for water purification. *Desalination* **1998**, *115* (1998), 285–294.
(12) Rajeshwar, K. I. J.G.; Swai, G. M. Electrochemistry and the environment. *J. Appl. Electrochem.* **1994**, *24*, 1077–1091.
(13) Chen, X.; Chen, G.; Yue, P. L. Novel electrode system for electroflotation of wastewater. *Environ. Sci. Technol.* **2002**, *36*, 778–783.
(14) Daneshvar, N.; Ashassi-Sorkhabi, H.; Tizpar, A. Decolorization of orange II by electrocoagulation method. *Sep. Purif. Technol.* **2003**, *31* (2), 153–162.
(15) Mollah, M. Y. A.; Morkovsky, P.; Gomes, J. A. G.; Kesmez, M.; Parga, J.; Cocke, D. L. Fundamentals, present and future perspectives of electrocoagulation. *J. Hazard. Mater.* **2004**, *114* (1−3), 199–210.
(16) Kobya, M.; Can, O. T.; Bayramoglu, M. Treatment of textile wastewaters by electrocoagulation using iron and aluminum electrodes. *J. Hazard. Mater. B.* **2003**, *100* (2003), 163–178.
(17) Llerena, C.; Ho, J. C. K.; Piron, D. L. Effects of pH on electroflotation of sphalerite. *Chem. Eng. Commun.* **1996**, *155* (1), 217–228.
(18) Shon, H. K.; Vigneswaran, S.; Kandasamy, J.; Kim, J. B.; Park, H. J.; Choi, S. W.; Kim, J. H. Preparation of titanium oxide, iron oxide, and aluminium oxide from sludge generated from Ti-salt, Fe-salt and Al-salt flocculation of wastewater. *J. Ind. Eng. Chem.* **2009**, *15* (5), 719–723.
(19) Jelks, B. *Titanium: Its Occurrence, Chemistry and Technology*; Ronald Press: New York, 1966.
(20) Serpone, N. Pelizzetti, E. *Photocatalysis: Fundamentals and Applications*; John Wiley & Sons: New York, 1989.
(21) Kaneko, M. Okura, I. *Photocatalysis: Science and Technology*; Springer: Tokyo, 2002.
(22) Gong, D.; Grimes, C. A.; Varghese, O. K.; Hu, W.; Singh, R. S.; Chen, Z.; Dickey, E. C. Titanium oxide nanotube arrays prepared by anodic oxidation. *J. Mater. Res.* **2001**, *16* (12), 3331–3334.
(23) Mora, G. K.; Varghesea, O. K.; Paulosea, M.; Shankara, K.; Grimes, C. A. A review on highly ordered, vertically oriented TiO_2 nanotube arrays: Fabrication, material properties, and solar energy applications. *Sol. Energy Mater. Sol. Cells* **2006**, *90* (14), 2011–2075.
(24) Shon, H. K.; Vigneswaran, S.; Kim, I.; Cho, J.; Kim, G. J.; Kim, J.-B.; Kim, J.-H. Preparation of functional titanium oxide (TiO_2) from sludge produced by titanium tetrachloride (TiCl4) flocculation of wastewater. *Environ. Sci. Technol.* **2007**, *41* (4), 1372–1377.
(25) Shon, H. K.; Vigneswaran, S.; Ngo, H. H. Effect of partial flocculation and adsorption as pretreatment to ultrafiltration. *AIChE J.* **2006**, *52* (1), 207–216.
(26) Seo, G. T.; Ohgaki, S.; Suzuki, Y. Sorption characteristics of biological powdered activated carbon in BPAC-MF (biological activated carbon-microfiltration) system for refractory organic removal. *Water Sci. Technol.* **1997**, *35*, 163–170.
(27) Moreno-Casillas, H. A.; Cocke, D. L.; Gomes, J. A. G.; Morkovsky, P.; Parga, J. R.; Peterson, E. Electrocoagulation mechanism for COD removal. *Sep. Purif. Technol.* **2007**, *56* (2), 204–211.
(28) Takeuchi, M.; Kimura, T.; Hidaka, M.; Rakhmawaty, D.; Anpo, M. Photocatalytic oxidation of acetaldehyde with oxygen on TiO_2/ZSM-5 photocatalysts: Effect of hydrophobicity of zeolites. *J. Catal.* **2007**, *246* (2), 235–240.
(29) Koyuncu, I. Reactive dye removal in dye/salt mixtures by nanofiltration membranes containing vinyl Sulphone dyes: effects of feed concentration and cross flow velocity. *Desalination* **2002**, *143* (2002), 243–253.
(30) Allegre, C.; Maisseu, M.; Charbit, F.; Moulin, P. Coagulation−flocculation−decantation of dyehouse effluents: Concentrated effluents. *J. Hazard. Mater.* **2004**, *116* (2004), 57–64.
(31) Kabdaşl, I.; Arslan-Alaton, I.; Vardar, B.; Tünay, O. Comparison of electrocoagulation, coagulation and the Fenton process for the treatment of reactive dyebath effluent. *Water Sci. Technol.* **2007**, *55* (2007), 125–134.
(32) Mollah, M. Y. A.; Schennach, R.; Parga, J. R.; Cocke, D. L. Electrocoagulation (EC)—Science and applications. *J. Hazard. Mater.* **2001**, *84* (1), 29–41.
(33) Suryanarayana, C. Nanocrystalline materials. *Int. Mater. Rev.* **1995**, *40*, 41–64.
(34) Irie, H.; Washizuka, S.; Hashimoto, K. Hydrophilicity on carbon-doped TiO_2 thin films under visible light. *Thin Solid Films* **2006**, *510*, 21.
(35) Shon, H.; Phuntsho, S.; Okour, Y.; Cho, D.-L.; Kim, K. S.; Li, H.-J.; Na, S.; Kim, J. B.; Kim, J.-H. Visible light responsive titanium dioxide (TiO_2). *J. Korean Ind. Eng. Chem.* **2008**, *19* (1), 1–16.

ES100333S